circle of Willis, cerebral arteries,
physical model, nonlinearity of flow

Krzysztof CIEŚLICKI*

EXPERIMENTAL AND NUMERICAL MODELLING OF FLOW IN THE HUMAN CEREBRAL ARTERIES

The paper presents the results of experiments concerning flow in the model of cerebral supplying arteries and the Circle of Willis (CW). Vascular phantom was prepared on the basis of anatomical specimens. The most typical artery shapes and dimensions were considered. Pressure distribution in 6 characteristic points is provided, and so are the average flow rates in the anterior, middle and posterior section of the brain. Tests were run in the conditions replicating the physiological state (i.e. when the supplying arteries were fully patent) and in pathological conditions, in which the internal carotid and vertebral arteries were occluded on one or both sides. Thus obtained results were compared with the results of computer simulations based on linear and non-linear flow models. To estimate the non-linear resistance of vascular segment two phenomenological formulae were proposed. High degree of correlation between the values obtained from experiments and those registered in non-linear computer model proves usefulness of proposed formulae. It verifies the hypothesis that nonlinearity of flow characteristics of the vessel segments is to a great extent caused by their tortuous and small length in relation to diameter. Non-linear effects are particularly pronounced in conditions of pathological occlusion of supplying vessels.

1. INTRODUCTION

Blood vessels supplying the human brain consist of two independent vascular systems: internal carotid arteries (ICA) and vertebral arteries (VA). Anterior and middle cerebral arteries are formed from internal carotid arteries. Vertebral arteries join to form the basilar artery (BA), which is soon divided into two posterior cerebral arteries. In the base of the brain both systems of vessels are connected bilaterally by posterior communicating arteries (PCoA) and left-to-right side by anterior communicating artery (ACoA) forming the so called Circle of Willis (CW). The main branches of the CW are segments of the anterior cerebral arteries (A2), the middle cerebral arteries (M2) and the posterior cerebral arteries (P2). The Circle of Willis is thought to have a major role in collateral circulation in the brain, both during physiological neck movements partially occluding the vessels supplying blood to intracranial regions and in pathological situations, for example in the case of obliterate atheromatosis in carotid arteries or in the vertebra-basilar system [12, 13, 14; 18]. Topography of supplying cerebral arteries and the circle of Willis is shown in Fig.1.

* Institute of Automatic Control and Robotics, Warsaw University of Technology, Boboli 8, 02-525 Warsaw, Poland

The anatomical specificity of cerebral arteries involves:

- presence of several nodes in which arteries join or bifurcate;
- spatial tortuous of internal carotid arteries and vertebral arteries.

In terms of hydrodynamics this is an extremely complicated flow system.

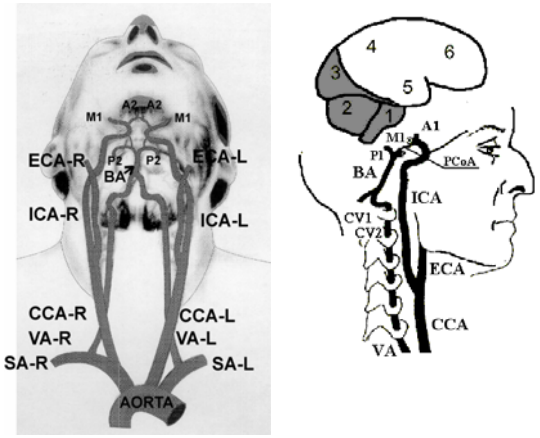

Fig. 1. Topography of cerebral supplying arteries and the Circle of Willis in front and side view

Physical nodes cause significant flow disturbances in their neighbourhood that result in velocity profile development along the outgoing branches. Developments of velocity profile proceed at a certain distance L_e, called the entrance region. Its value is proportional to the vessel's diameter d and the Reynolds number Re according to the relation $Le \cong 0.07\, d\, Re$ [2, 9]. As many arteries in the base of the brain are relatively short, the entrance region may cover their entire length.

Tortuous of channels, in turn, gives rise to centrifugal forces. In a single bend, centrifugal force acting towards the outer wall of a bend deforms axial (initially parabolic) inlet velocity profile and develops the secondary flow which has the form of two vortices rotating in opposite direction. The resultant flow is helical in both halves of the tube [1, 8, 24]. Mixing action of the secondary flow prevents an increase in the boundary layer thickness and also prevents the flow separation. As a result, the inlet section where the velocity profile is formed gets shorter.

Due to both discussed hydrodynamic effects pressure-flow relations in arterial segments are non-linear. Thorough study of the literature on the subject, as well as this author extensive theoretical and experimental investigations have lead to the conclusion that the relation between the volume flow rate Q and the pressure drop Δp within the laminar flow regime will best be given by the formula:

$$\Delta p = AQ + BQ^n \qquad (1)$$

The first term AQ expresses the main, linear component of pressure drop. The second term BQ^n expresses additional pressure lost due to segment tortuousity or velocity profile development. The value of exponent n may be either 1.5 or 2. The former value concerns tortuous arterial segments, the latter concerns straight, relatively short segments [5]. Coefficients A and B depend on morphometry of the given vessel.

2. MATERIALS AND METHODS

2.1. PHYSICAL MODEL OF FLOW IN THE CIRCLE OF WILLIS

The wax model of cerebral supplying vessels was made by neurosurgeons and anatomists on the basis of microsurgical anatomy of tens of specimens of vertebral-basilar and internal carotid arteries [17, 19, 20, 21], as well as of the CW [15, 16]. Dimensions of individual segments of the model remained within the range of accessible anatomical results. The wax model is presented in Fig. 2a in oblique view which show spatial complexity and tortuous of the vessels.

The transparent phantom of brain-supplying arteries was made of polyurethane material PX-515 on the basis of wax model [6]. It consisted of two parts imitating the vertebra-basilar system and the internal carotid system of arteries. To obtain the vascular phantom, both parts of the wax model were placed in Plexiglas moulds which were then filled by a mixture of monomer and an initiator. When the polymerisation process was completed, the resulting blocks were dried in a laboratory drier to make the wax ooze. Both parts of the vascular phantom were then interconnected with external straight capillaries modelling the posterior communicating arteries. The wax model of the vertebro-basilar system of vessels and its final vascular phantom is shown in Fig. 2b,c.

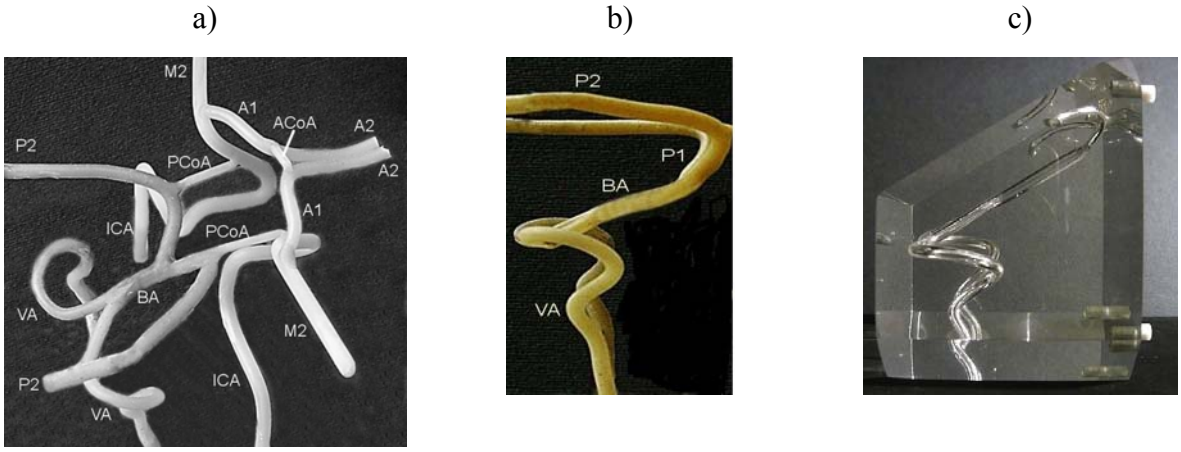

Fig. 2. a) Oblique view of wax model of blood vessels supplying the brain; b) wax model of the vertebro-basilar system; c) transparent vascular phantom of the vertebro-basilar system

The peripheral resistances of the anterior, middle and posterior parts of the brain were modelled by straight tubes of precisely controlled length and diameter to ensure the proper redistribution of flow between all the outlet branches. Their values equal to: 60, 30 and 42 mmHg*s/ml, accordingly, were taken to be inversely proportional to the mass of the brain section which they supply [11]. The dimensions of all vascular segments as well as capillaries which simulate posterior communicating arteries are given in Table 1.

The experimental set-up is shown in Fig. 3 [7]. The applied liquid was the water-solution of glycerine with the viscosity of 3.5 mPas. Flow intensity was induced by a computer-controlled variable rate pump. Both in physiological and pathological situations,

the average flow intensity were chosen to secure an inlet pressure range of between approximately 80 mmHg and 120 mmHg.

Table 1. Model dimensions

Vessel	Left side			Right side		
	l [mm]	d [mm]	a_K [mm]	l [mm]	d [mm]	a_K [mm]
ICA	142	3.6	5	144	3.6	5
VA	125	2.5	8	130	2.5	8
BA	28	3.3	-			
A1	20	2	10	20	2	10
P1	13	2	8	11	2	8
A2	45	2	10	45	2	10
M1	51	3	15	42	3	15
P2	60	2	10	65	2	10
PCoA	15	1	-	15	1	-
ACoA	6	1	15			

The mass rates of flow ρQ in all branches of the CW were measured with an accuracy of approximately 2% by weighing the mass of liquid which left the individual outlet of the model within a time interval which was the multiple of the period of the first harmonic of the induced flow rate (equal to 1Hz).

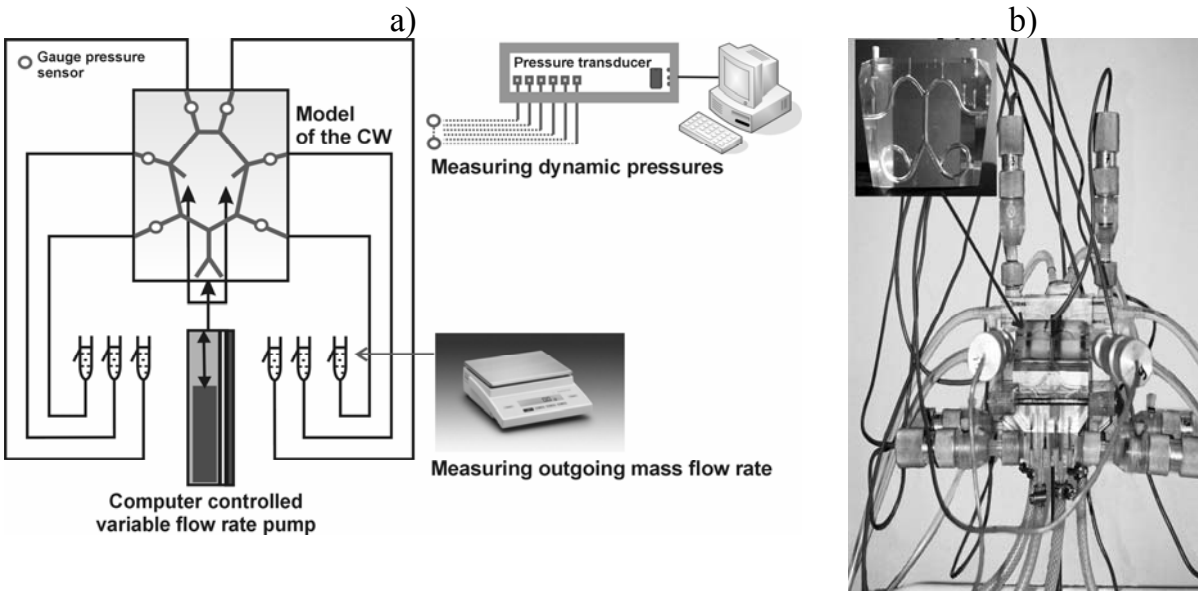

Fig. 3. a) Experimental set-up for measuring pressure and flow rate distributions;
b) Photograph of the transparent vascular phantom with the pressure gauges.

Pressure measurements with accuracy of approximately 1.5% were taken with the pressure transducers at 10 points. Six of them were situated in all branches of the CW, 10 mm downstream from arterial nodes, while the remaining four were positioned 10 mm downstream from the inlet of all supplying arteries. Pressure data recording and storing was

done using own software controlling the A/D card. Constant outlet pressure was maintained and adjusted by means of six small overflow reservoirs provided at the far ends of the model and located at the same height (Fig. 3).

2.2. LINEAR/NON-LINEAR COMPUTER MODEL OF FLOW IN THE CIRCLE OF WILLIS

Using flow-electric analogy, the hydraulic model was depicted as an electric circuit consisting of alternative linear or non-linear elements. Its non-linear version is shown in Fig. 4a.

It is a network including 10 nodes connecting 18 arterial segments. Because the experiments were performed on rigid vascular phantom, all the simulated impedances are purely resistive. The individual resistance of each segment was denoted by a symbol derived from an abbreviated form of its anatomical name. Peripheral resistance was marked by the symbol P followed by the abbreviation indicating the brain part. The network was presented as a SPICE net list (Simulation Program with Integrated Circuit Emphasis) and was then solved using widely applied industry standard PSpice procedures – Cadence PSD 14.2. This made possible the calculation of flows in all branches of the CW as well as pressure values in all points corresponding to sensor locations (marked by open circles in Fig. 3).

The hydraulic resistances of all elements of the linear model were derived from the Hagen-Poiseuille's (HP) formula and hence were independent of the flow velocity. To obtain their numerical values, the geometrical dimensions given in Table 1 were used.

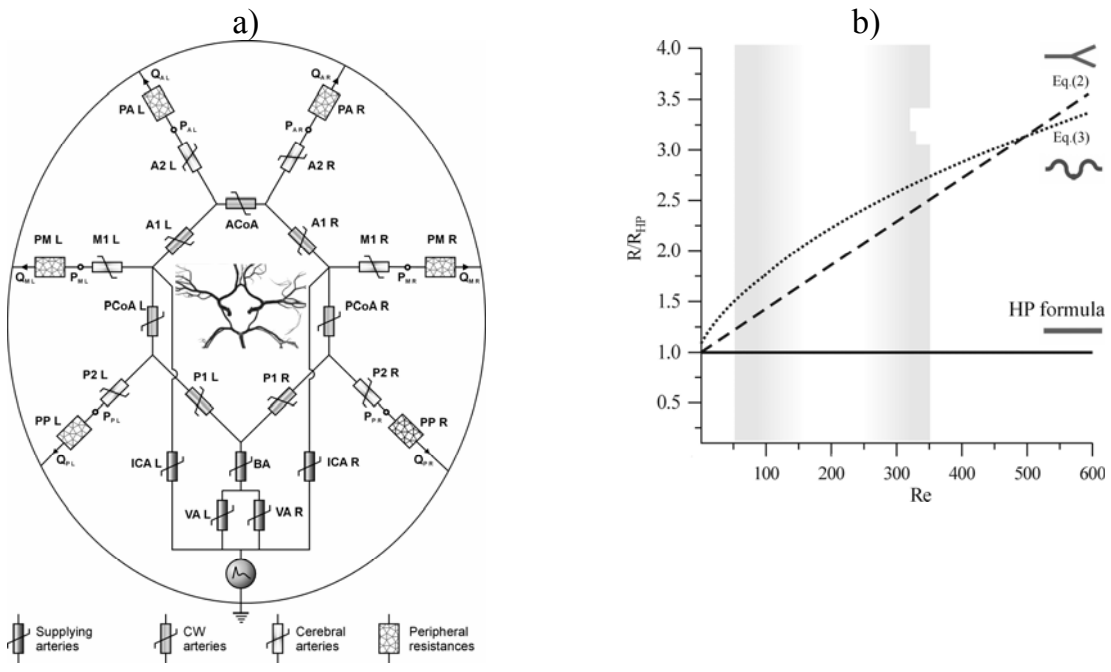

Fig. 4. a) Electric model of the Circle of Willis; b) Sketches of equations (2) and (3) in the dynamic state and within the range of *Re* number typical for physiology, for exemplary values $a/a_K = 0.36$ and $d/l = 0.1$.

The resistances of vessel segments (R_l, or R_t) in the non-linear model were derived from the formula (1) and then normalised by the value obtained from the HP formula (R_{HP}).

They are functions of the Reynolds number $(Re = 4Q/(\pi d \nu))$ (in which ν denotes kinematical coefficient of viscosity) and have forms [5]:

$$\frac{R_l}{R_{\mathrm{HP}}} = 1 + 0.044 \frac{d}{l} Re \qquad (2)$$

$$\frac{R_{\mathrm{t}}}{R_{HP}} = 0.526 + \sqrt{0.225 + 0.022 \sqrt{\frac{a}{a_K}} Re.} \qquad (3)$$

Equation (2) concerns short arterial segments, in which velocity profile development is of primary importance. As we can see, the hydraulic resistance of segment of a finite length increases linearly with the mean flow rate and the greater the segment diameter to length ratio, the faster the increase. Equation (3) concerns tortuous segment with the cross-section radius a and the bend curvature radius a_K. The product $\left(\sqrt{a/a_K} \cdot Re\right)$ is called Dean's number (Di) and it plays a comparable role to that of the Re number for straight pipes [8]. Research work described in few publications [3,4] revealed that flow characteristics for segments equal in length in diameter, though bent differently, will be very similar as long as the curvature radius a_{K} is nearly the same. For $Re \to 0$, the values of both equations tend to a constant value approximately equal to 1.

Sketches of equations (2) and (3) in the dynamic state and within the range of Re number typical for physiology, for exemplary values $a/a_K = 0.36$ and $d/l = 0.1$, are presented in Fig. 4b. As can be seen, the non-linear flow resistance is approximately 1.5 to 3 times larger than the linear flow resistance calculated from the HP formula. The most rapid increase of flow resistance concerns curved segments.

In non-linear model of flow in the CW, the hydraulic resistance of short and straight vessels, such as the basilar artery and posterior communicating arteries, was obtained from (2) and the resistance of the remaining, spatially bent arteries was obtained from (3).

2.3. PERCENT DEVIATION BETWEEN MODELS

For quantitative estimation of quality of mapping the real flows and pressures distributions by non-linear or linear computer models the average distance between measured and simulated quantities were calculated using the formula:

$$\delta = \frac{1}{6} \sum_{i=1}^{6} \left| V_{i,E} - V_{i,M} \right|, \qquad (4)$$

in which $V_{i,E}$ refers to average pressure or flow rate value obtained from experiment in the i-th model branch, whereas $V_{i,M}$ refers to the relevant value obtained from the modelling.

3. RESULTS

Only three extreme cases from all the tests conducted are presented in this paper:

I. Patency of all supplying vessels;
II. Occlusion of the left carotid artery;
III. Complete occlusion of the vertebral-basilar system and the left carotid artery.

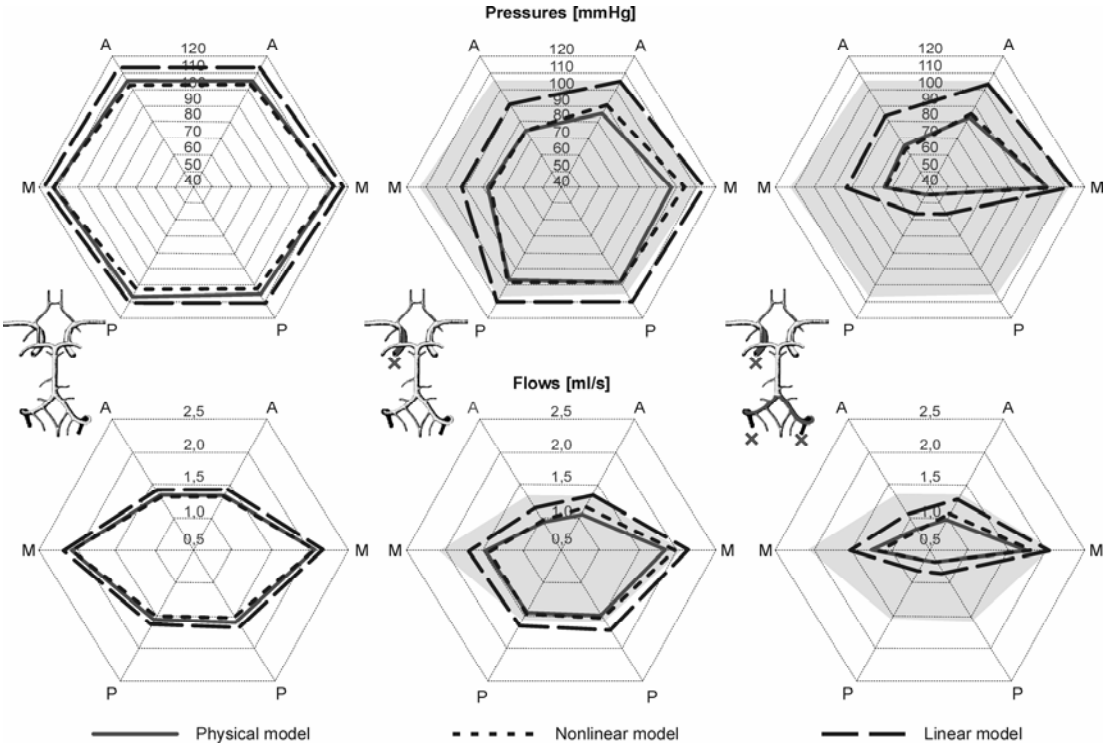

Fig. 5. Comparison of results of experiments (physical model) and blood flow simulations for the nonlinear and linear model in conditions of: I - patency of all supplying vessels, II - occlusion of the left ICA, III – complete occlusion of the VBA system and the left ICA. Physiological pressure and flow rate values in cases II and III are highlighted

The average pressure values (in mm Hg) as well as the average flow rates (in ml/s) measured in the physical model were contrasted with those obtained from non-linear and linear computer models and presented on circular graphs which symbolise their spatial distribution. They are presented in Fig. 5. The highlighted areas in cases II and III correspond to the physiological pressure and flow rate distributions.

The δ_1 values calculated in accordance with formula (4) for all cases are shown in Table 2.

Table 2. Average errors between physical and computer models

Case	Flows [ml/s]		Pressures [mmHg]	
	Nonlinear	Linear	Nonlinear	Linear
I	0.03	0.11	2.4	7.0
II	0.07	0.28	3.0	18.2
III	0.05	0.29	1.2	18.8

As results from Table 2 the flow and pressure distributions in cerebral arteries are mapped by non-linear model with the average accuracy of 0.03 ml/s (flows) and 2.4 mmHg (pressures) in case of patency of all supplying arteries (Fig. 5 left). The same parameter calculated for linear model is about three times higher. It is, nevertheless, still satisfactory.

In pathological situations caused by occlusion of the left carotid artery or occlusion of the vertebro-basilar system and left carotid artery, the observed differences increase significantly. In the first place they refer to the pressures measured. In linear models the maximum distance from experimental values reaches as much as 16.7 mmHg (in situation of the one side occlusion of ICA). In the non-linear model maximum distance does not exceed 5.1 mmHg. Table 2 highlights growing inadequacy of linear models in comparison to the non-linear one with increasing number of occluded vessels (single ICA $\rightarrow$ both VA and ICA). In the third case, the average difference between physical and linear model is about 6 times higher (for flows) and 16 times higher (for pressures) than in the non-linear one.

4. DISCUSSION OF RESULTS

In the majority of opinions, the differences between the linear and non-linear models are not physiologically significant due to the approximately 1:20 baseline proportion of resistance between the proximal and distal parts of cerebral circulation [22]. Experiments showed however, that this might be true only in the physiological case, when all supplying arteries are fully patent. In pathological cases, when the internal carotid or vertebral arteries are occluded on one or both sides, the linear model leads to a significant overestimation of pressure and flow rate values at the level of the CW. In qualitative terms this results seems well justified, since the occlusion of brain-supplying vessels gives rise to the compensating flow through the short anatomises (ACoA and/or PCoA) of the CW and, at the same time, causes an increase of the flow rate in the remaining supplying vessels. In the physical and non-linear models it leads to a major increase in the hydraulic resistance of the segments, which results in a more pronounced pressure drop. When the blood-supply pressure is maintained, this effect is revealed as a flow rate reduction in the cerebral arteries which is more marked than in the linear model. That is why pressure and flow graphs, obtained for physical and non-linear models, always remain inside the linear ones.

One can assume that nonlinearity of arteries resistance might prove beneficial in the conditions of the mean arterial pressure drop. In the linear model a decrease of the driving pressure is accompanied by a proportional flow rate reduction. In non-linear models this effect is vastly reduced because of the decreasing resistance of the brain-supplying arteries.

Vessel compliance and the cerebral auto regulation mechanism could be easily incorporated into the electrical model presented here. Such a model would, however, contain considerably more parameters, the identification of which is uncertain, as in a live organism they are subject to continuous functional adaptations.

Vessels compliance would not affect the average values of pressure and flow rates presented in this study. As far as the auto regulation is concerned, we may speculate that it would partly compensate for the effects of occlusion and the rate of the total cerebral flow would be higher than in Fig. 5. However, because of strong nonlinearities of supplying

arteries resistance, the pressure drop would be more significant than that calculated for the physical model. Accordingly, pressures at the CW level that is at the entry of cerebral vascular territories would be lower still, tending to the lower limit of auto regulation.

It should be stressed, that presented model is 0-dimensional, and so it neglects spatial flow patterns and wall shear stress distribution in complex arterial geometries. Recently, calculations of 3D velocity fields in arteries have dominated the fluid dynamical study of blood flow and were driven by the need to understand the link between wall shear stress and the development of arterial disease [10]. Atherosclerosis is the main cause of death in the Western world, no wonder why so many studies are devoted to this problem.

To calculate 3D velocity field in the considered arterial cerebral network, we would have to solve the full set of nonlinear partial differential Navier-Stokes equations. Although there are a number of commercial numerical tools utilising body-fitted coordinates and a finite volume discrimination procedure [23] we did not follow that way, mainly due to the difficulty in grasping such type of model by doctors and long calculation time.

The presented approach to cerebral blood flow modelling might be named "topological", as only the branch flow rates and nodal pressures in the considered arterial network were evaluated. Although such approach is incomparably simpler than the "field approach", it enables quick estimation of pressure values at the Circle of Willis level with accuracy sufficient for physiology so long as basic dimensions and curvature radius of individual arterial segments are known. Estimation of value of the above mentioned pressure is of clinical importance. It determines cerebral perfusion as well as the auto regulation pressure reserve. From obvious reasons its value may not be measured *in vivo*.

5. CONCLUSIONS

A high degree of correspondence of the pressure and flow values registered in the physical and non-linear computer model proves the usefulness of the proposed formulae (2) and (3) in estimating the nonlinear resistance of the vascular segment and verifies the hypothesis that nonlinearity of flow characteristics of the vessel segments are, to a great extent, caused by their tortuous and small length in relation to their diameter.

The experiments confirmed a relatively good tolerance of a human organism to one-sided occlusion of the internal carotid artery. This fact is well known from clinical observations. Two-sided occlusion of vertebra-basilar system together with unilateral flow deficiency in the carotid arteries leads to major disturbances in the modelled circulation.

BIBLIOGRAPHY

[1] BANERJEE RK, CHO YI, BACK LH, Numerical Studies of Three-Dimensional Arterial Flows in Reverse Curvature Geometry: Part I – Peak Flow, Trans. ASME. J. Biomech. Eng., Vol. 115, pp.316-326, 1993.

[2] BOVENDEERD, P.H.M., STEENHOVEN, A.S.A., VAN VOSSE, F.N., VOSSERS, G., Steady Entry Flow in a Curved Pipe., Journal of Fluid Mechanics, Vol. 177, pp.505-510, 1987.

[3] CIESLICKI, K., LASOWSKA, A. SMOLARSKI A.Z., The influence of channel tortuousity on hydraulic resistance. Bulletin of the Polish Academy of Science series: Earth Science, Vol. 48, pp.161-173, 2000.

[4] CIESLICKI, K., LASOWSKA, A., SMOLARSKI, A.Z., Pressure-Flow Relation of Arterial Segments of Variable Geometry. Polish Journal of Medical Physics and Engineering Vol. 6, pp.55-67, 2000.

[5] CIESLICKI, K., Hydrodynamic conditions of cerebral circulation. Academic Press EXIT, Warszawa, 2001, (in Polish).

[6] CIESLICKI K., CISZEK B., LASOWSKA A., SMOLARSKI A. Z.: Modeling of flow in a network structure of the main cerebral arteries, *Bulletin of the Polish Academy of Science, seria:* Biological Science, Vol. 50, pp.25-35, 2002.

[7] CIESLICKI K., CIEŚLA D., Studies of flow in the physical model of the main supplying and cerebral arteries, Proc. IASTED International Conference on Biomedical Engineering (BioMED), pp.49-52, Innsbruck, 2004.

[8] DEAN, W.R., Note on the motion of fluid in a curved pipe, Philosophical Magazine, Vol. 7, pp.208-223, 1927.

[9] DU PLESSIS, J.P., KROEGER, D.G., Hydrodynamical entrance length effects for ducts flow with arbitrary inlet velocity profiles. Transactions ASME, Journal of Applied Mechanics, Vol. 51, pp.239-243, 1984.

[10] FRANGOS S. G., GAHTAN V., STUMPIO B., Localization of Atherosclerosis. Role of Hemodynamics, *Arch. Surg.* Vol. 134, pp.1142-1149, 1999.

[11] HILLEN, B., DRINKENBURG, B.A., HOOGSTRATEN, H.W., POST, L., Analysis of Flow and Vascular Resistance in a Model of the Circle of Willis, Journal of Biomechanics, Vol. 21, pp.807-814, 1988.

[12] HILLEN, B., HOOGSTRATEN, H.W., VAN OVERBEEKE, J.J., VAN DER ZWAN, A., Functional anatomy of the circulus arteriosus cerebri (Willis), Bulletin de l'Association des Anatomistes, Vol. 75, pp.123-126, 1991.

[13] HOKSBERGEN A.W.J.; FULESDI B., LEGEMATE D.A., CSIBA L., Collateral Configuration of the Circle of Willis. Transcranial Color-Coded Duplex Ultrasonography and Comparison With Postmortem Anatomy, Stroke, Vol. 31, pp.1346-1351, 2000.

[14] KLUYTMANS M., VAN DER GROND J., VAN EVERDINGEN K.J., KLIJN C.J.M., KAPPELLE L.J., VIERGEVER M.A., Cerebral Hemodynamics in Relation to Patterns of Collateral Flow. Stroke, Vol. 30, pp.1432-1439, 1999.

[15] KWOLEK-KLIMKIEWICZ, J., CISZEK, B., ALEKSANDROWICZ, R., MAZUROWSKI, W., ZABEK, M., GORSKI, R., Microsurgical anatomy of the anterior communicating artery. Folia Morphologica, Vol. 55, pp.369-370, 1996.

[16] KLAPECKI J, PACHOLEC E, CISZEK B, Anatomy of the posterior communicating artery - preliminary report, Folia Morphologica, Vol. 55, pp.335-337, 1996.

[17] LELEN M., CISZEK B., ZABEK M., KRAJEWSKI P., CIESLICKI K., Anatomy of the pontine part of the cerebellar arteries and large basilar artery pontine branches, Medical Science Monitor, Vol. 4(supp. 2), pp.28-30, 1998.

[18] LIEBESKIND D.S., Collateral Circulation, Stroke, Vol. 34, pp.2279-2284, 2003.

[19] MICHALIK, R., CISZEK, B., ZABEK, M., MARCHEL, A., Anatomy of distal division of the basilar artery, Przegląd Lekarski, Vol. 33, pp.107-100, 1996, (in Polish).

[20] MICHALIK, R., CISZEK B., ZABEK M., MAZUROWSKI W., ALEKSANDROWICZ R., Microsurgical anatomy of the final division of the basilar artery, Folia Morphologica, Vol. 55, pp.363-395, 1996.

[21] PACHOLEC, E., CISZEK, B., Morphometry of the supraclinoid part of the internal carotid artery, Acta Clinica, Vol. 2, pp.96-101 2003, (in Polish).

[22] PIECHNIK, S., CIESLICKI, K., CIESLA, D., CZOSNYKA M., Problems n Application of Purely Linear Models in Cerebral Circulation, Journal of Biomechanics, Vol. 35, pp.553-554, 2002.

[23] SHIPKOWITZ T, RODGERS V. G. J., FRANZIN L. J., CHANDRAN K. B., Numerical study on the effect of steady axial flow development in the human aorta on local shear stresses in abdominal aortic branches, Journal of Biomechanics, Vol. 31, pp.995-1007, 1998.

[24] VAN DYKE M, Extended Stokes Series: Laminar Flow through a Loosely Coiled Pipe, Journal of Fluid Mechanics, Vol. 86**,** pp.29-145, 1978.